Materials
Views
www.MaterialsViews.com

ADVANCED
MATERIALS
www.advmat.de

COMMUNICATION

Liquid-Phase Metal Inclusions for a Conductive Polymer Composite

Andrew Fassler and Carmel Majidi*

We introduce a soft and highly stretchable elastomeric film (**Figure 1**a,b) that becomes permanently conductive upon the application of concentrated compressive stress (Figure 1c–f). Referring to **Figure 2**a–d, the conductive elastomer is composed of a thin sheet of poly(dimethylsiloxane) (PDMS) embedded with microscopic inclusions of liquid-phase gallium–indium–tin ("galinstan"; electrical conductivity, $\sigma = 3.46 \times 10^6$ S m^{-1}, melting point $= -19$ °C)[1] droplets. The PDMS–galinstan composite is not initially conductive, but concentrated surface pressure causes a permanent change in the material's structure and bulk properties, resulting in a volumetric conductivity of $\sigma = 1.05 \times 10^4$ S m^{-1}. Because of this, it is possible to selectively induce conductivity in a sheet of the material, allowing simple circuits to be drawn onto a sample (Figure 1c,f and Video S1 and S2, Supporting Information). Since the conductive inclusions are liquid-phase, the bulk material is still highly soft (Young's modulus, $E = 0.90$–1.27 MPa) and elastic, with a strain to failure of $\varepsilon_f = 133\%$ strain (i.e., over twice its natural length). The modulus of the composite is similar to that of natural human skin (0.4–0.8 MPa[2]) and an order-of-magnitude less than striated muscle (≈ 10–50 MPa.[3,4]) This biomechanical compatibility allows the material to easily conform to the contours of the human body and stretch as the body moves. Additionally, while under tension the resistance remains approximately constant so that the properties of the circuit are unaffected. Compared with other conductive elastomers with similar modulus (i.e., carbon black–PDMS and Ag–PDMS with $E \approx 1$ MPa[5–7]), this PDMS–galinstan composite exhibits orders of magnitude greater volumetric conductivity (Figure 2e).

High compliance (low E) and elasticity (high ε_f) represent key challenges in the development of mechanically robust electronics that are compatible with natural human tissue for wearable computing, implantable devices, and physical human–machine interaction. Presently, soft and stretchable functionality can be introduced through so-called "deterministic" architectures in which thin flexible circuits are bonded to an elastomer substrate and buckled or patterned into wavy/serpentine planar geometries. This approach has been successful in tissue and skin mounted sensors,[8,9] stretchable batteries,[10]

and hemispherical cameras.[11] Alternatively, solid metal wiring can be replaced with metal alloys that are liquid at room temperature. This approach has been utilized to create a variety of strain, curvature, and pressure sensors,[12–14] antennas,[15,16] dielectric elastomer actuators,[17] and memristors.[18] Liquid-phase gallium–indium alloys are popular for this "microfluidics" approach to stretchable electronics since they are non-toxic and form an oxide layer[19–22] that aids in microcontact printing,[23] electrode alignment,[24] and 3D printing.[25] Finally, a common approach to stretchable electronics is to embed thin films of elastomer with a percolating network of conductive particulates, such as structured carbon black,[26] carbon nanotubes,[27–30] silver nanoparticles,[31,32] silver nanowires,[33] and graphene.[19,28] In contrast to deterministic and microfluidic architectures, such micro- and nanocomposites exhibit isotropic conductivity at virtually all length scales and can be rapidly patterned into circuits with screen printing, stencil lithography, microcontact printing, or additive manufacturing. However, as shown in Figure 2e, their volumetric conductivity is poor compared with bulk conductors and improving conductivity by increasing the weight% of conductive filler increases the mechanical stiffness and brittleness of the composite.[34,35]

As a conductive filler, liquid-phase metal alloy represents an ideal alternative to rigid particulates that introduces volumetric conductivity through percolation without increasing the stiffness and brittleness of the elastomeric composite. The conductive elastomer is prepared by mixing galinstan (Ga 68.5%, In 21.5%, Sn 10% by weight; GalliumSource, LLC) with PDMS (Sylgard 184; Dow Corning Corporation) using a mortar and pestle. The ratio of the two materials is 1:1 by volume (6.6:1 galinstan to PDMS by weight) and they are mixed until the galinstan droplets are 2–30 µm in size (Figure 2b,c). Because of its relatively high concentration, the galinstan exhibits uniform dispersion and remains suspended within the PDMS despite their dramatically different densities. As an alternative to galinstan, eutectic gallium–indium (75% Ga, 25% In; EGaIn) can be used. Both alloys are nontoxic and exhibit similar electrical and rheological properties.[1] Galinstan was chosen for its lower off-the-shelf price. We have also explored mixing and dispersion through sonication, which is less labor intensive but requires more time for sample preparation (Supporting Information). After curing on a hotplate at 150 °C, the droplets of galinstan are temporarily encapsulated in closed-cell foam-like matrix of PDMS. In this bulk virgin state, the closed-cell geometry prevents conductivity between adjacent liquid metal inclusions. However, applying concentrated mechanical load, most notably through localized compression, causes the elastomer to exhibit volumetric conductivity. We postulate that this is caused by tearing or rupture of the foam cell walls and the formation of

A. Fassler, Prof. C. Majidi
Soft Machines Lab
Department of Mechanical Engineering
Carnegie Mellon University
Pittsburgh, PA 15213, USA
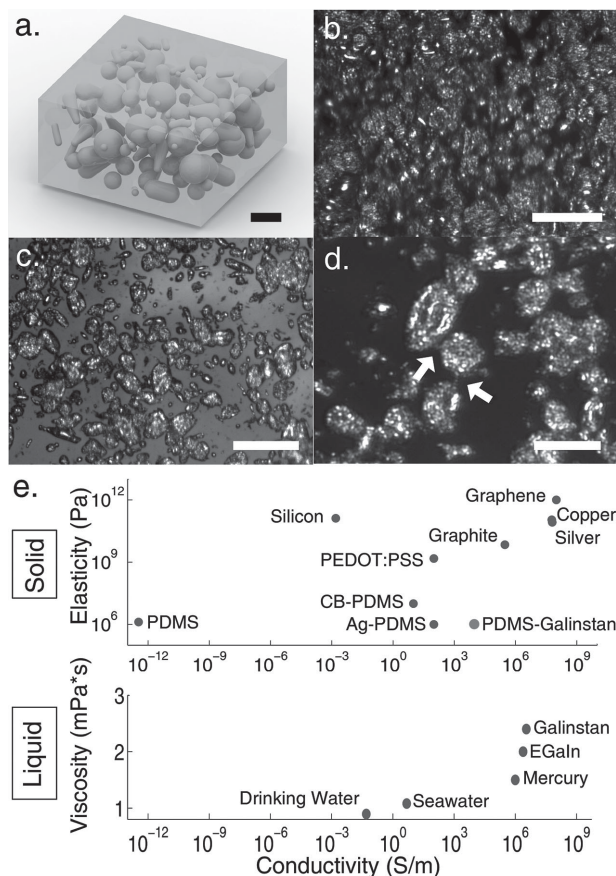E-mail: cmajidi@andrew.cmu.edu
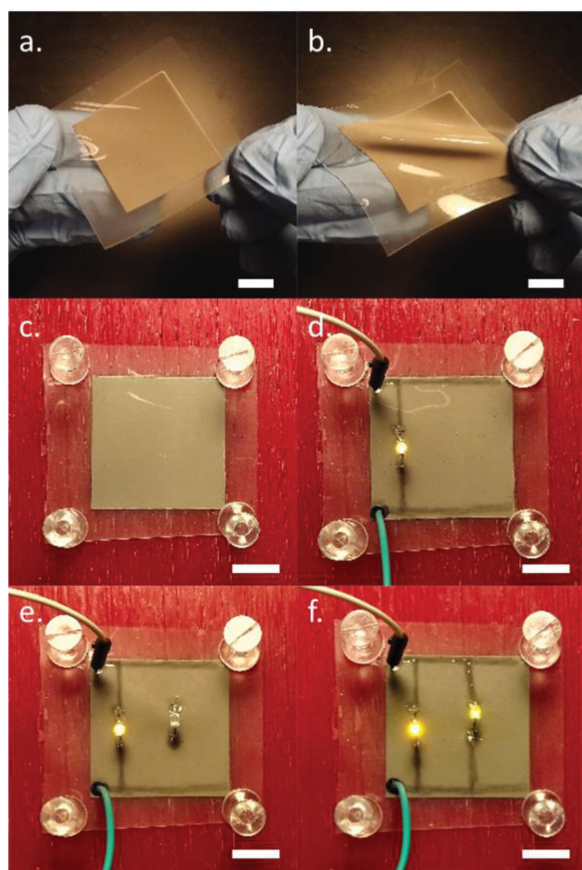
Figure 1. A square sheet of the stretchable PDMS–galinstan embedded in a thin layer of PDMS (a–c). Circuits can be drawn into this plain sheet of material (c) by using a thin tipped tool to selectively apply compression. An LED embedded into the nodes of a drawn circuit lights up (d), but a newly added LED will not (e) until more selective compression is used to draw connections to the existing circuit (f). Compression causes the material to darken, allowing the drawn conductive traces to be visible. Scale bar = 10 mm for all pictures.

Figure 2. a) Illustration of composite (scale bar = 25 µm). b) Microscope image of the PDMS–galinstan material; galinstan droplets are densely packed inside a clear PDMS matrix (scale bar = 50 µm). c) Monolayer of galinstan droplets; droplets are well distributed and exhibit a spheroidal shape with dimensions ranging from 2 to 30 µm (scale bar = 50 µm). d) Compression is believed to cause droplets to rupture and form electrical connections with neighboring inclusions (arrows) and leading to bulk conductivity (scale bar = 25 µm). e) Volumetric conductivity versus mechanical rigidity for various materials.

a continuous network of galinstan droplets (Figure 2d). Similar mechanisms for liquid GaIn conductivity have previously been examined for self-healing circuits.[36] In contrast to prefabricated open-cell polymer nano-networks,[37] the PDMS–galinstan composite presented here has no predefined foam structure and can be patterned for selective conductivity through the application of concentrated surface pressure.

We examine the pressure-controlled transition from the nonconductive virgin state to a permanently conductive state by compressing specimens using a 3.2 mm diameter cylindrical probe and measuring the resistance through the axis of loading. As samples are thin (0.50 mm), we are assuming that the area of induced conductivity is the area of the probe. On average, conductivity is initiated with a surface pressure of 1.7 MPa (n = five samples). Increasing the compressive stress causes the conductivity to monotonically increase due to further degradation of the closed-cell matrix structure. The relationship between this past largest compression and the resistance through the thickness of an individual sample can be seen in Figure S1a, Supporting Information. In addition to concentrated loading,

conductivity can also be permanently induced by pressing and rolling a rigid cylinder into the sample, altering the electrical properties of the entire specimen. In both cases, compression causes the material to darken and trace amounts of galinstan are sometimes observed to appear on the surface. Coating the material in a thin layer of PDMS prevents this outflow of the liquid metal. Tension can also induce conductivity, but this occurs at very large strains that are close to the failure limit ε_f of the material, with samples often tearing before the electrical behavior changes. Once compressed, the conductivity of the PDMS–galinstan composite is 1.05×10^4 S m^{-1} and exhibits unique electromechanical coupling.

When loaded in tension, the electrical resistance R through the length of a given specimen undergoes only modest increase, which implies that the volumetric conductivity $\sigma = L/RA$ increases significantly with load (**Figure 3**a–d). Here, L is the stretched length of the specimen and A is its cross-sectional area. Since it is entirely composed of incompressible fluid and elastomer (with no observed voids or air pockets), the
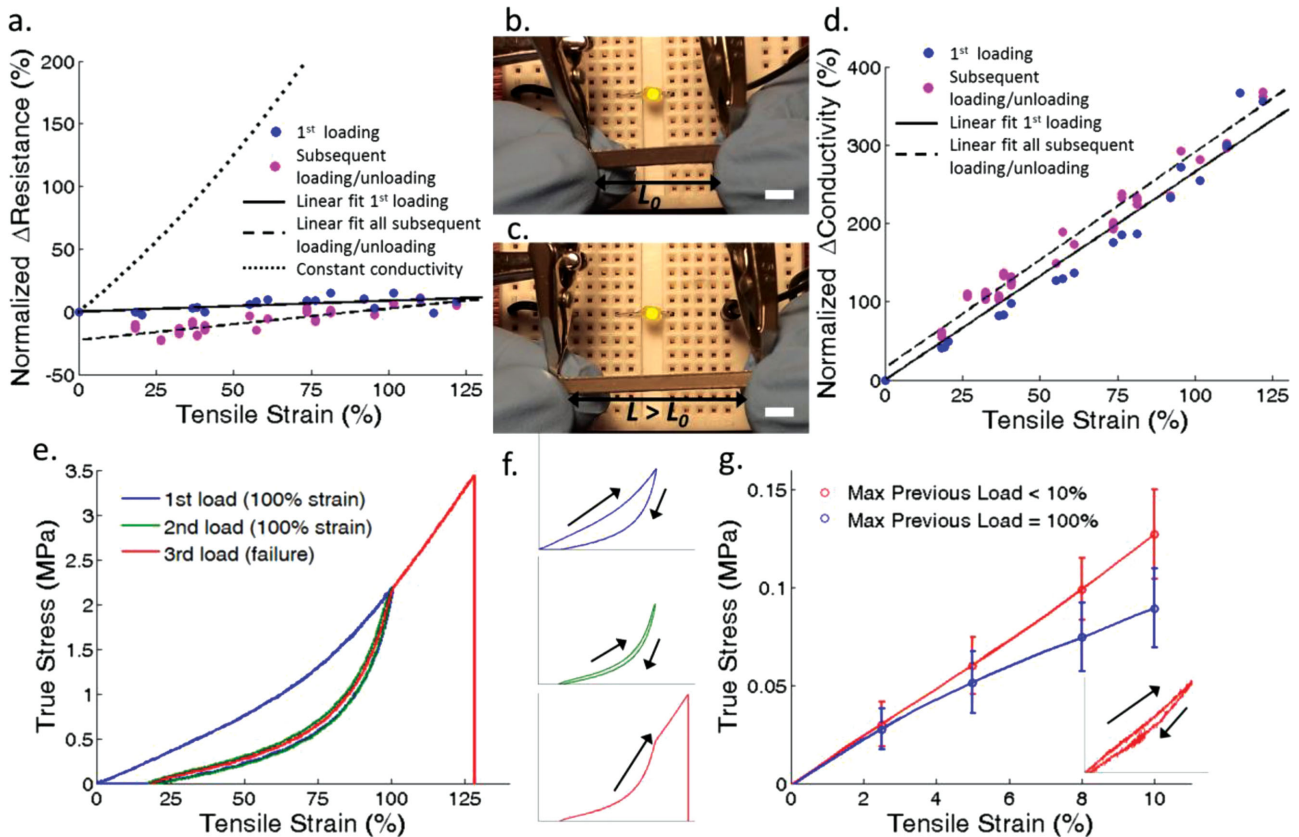
Figure 3. a) The relative change in resistance $\Delta R/R_0$ of PDMS–galinstan (previously compressed to induce conductivity) due to tensile strain ε is minimal, even at high strains. This is dramatically different from what would be predicted given constant volumetric conductivity σ and incompressibility (dotted line). Because of this, the operation of a LED circuit is unaffected by strain (b,c) (scale bar = 5 mm). d) The relative change $\Delta\sigma/\sigma_0$ volumetric conductivity (S m^{-1}) increases monotonically with ε. e) Tensile loading and unloading of a single specimen multiple times changes its mechanical properties, dependent on the max previous strain, these individual loading cycles separated in (f). g) This hysteresis effect is also seen when comparing the averaged tensile test data for specimen previously loaded to <10% strain and specimen loaded to 100% strain. The error bars display two standard deviations of the data. The inset shows a virgin sample loaded and unloaded to 10% strain, showing significantly less hysteresis than observed with larger stretch.

composite is assumed to be incompressible, which implies that $A = A_0/\lambda$, where $\lambda = L/L_0$ is the stretch and L_0 and A_0 are the natural (unloaded) length and cross-sectional area of the specimen. In contrast, a homogenous material with a constant bulk conductivity $\sigma = \sigma_0$ would exhibit a relative increase in electrical resistance $\Delta R/R_0 = \lambda^2 - 1$, where $R_0 = L/\sigma_0 A$ is the resistance of the specimen prior to stretch (dotted line in Figure 3a). The invariance of $\Delta R/R_0$ to stretch that we observe with the composite suggests that the conductivity is achieved through a preserved network of electrical contacts between embedded galinstan droplets. Three samples were elongated to 30 mm four times, with repeated stretching showing only a modest increase in conductivity. The greatest change in volumetric conductivity occurred after the first loading, with the dependence of σ on λ remaining similar in the subsequent unloading and loading of a sample. This is demonstrated in comparing plots of $\Delta R/R_0$ (Figure 3a) and $\Delta\sigma/\sigma_0 = (R_0/R)\lambda^2 - 1$ (Figure 3a) versus tensile strain $\varepsilon = \lambda - 1$ for loading during the first extension with responses during unloading after first extension and elongation/unloading of the second, third, and fourth extensions. One possible explanation is that the initial loading further degrades

the polymer's formerly closed cell structure, or otherwise redistribute the galinstan into a more stable and continuous configuration within the network (after which subsequent loadings have negligible effect). Successive loading of a sample to 35% strain for 50 cycles elicits stable resistance, with minimal difference between the loaded and unloaded resistance (Figure S1b, Supporting Information).

Tensile tests were performed on the PDMS–galinstan composite and reveal highly non-linear elastic deformation. As before, the assumption of incompressibility is used to calculate cross-sectional area and true stress. Large strains (100%) of a virgin specimen show strain hardening while loading, with a dramatic decrease in mechanical resistance during unloading (Figure 3e,f). Interestingly, if the sample is reloaded to this same high strain, the stress–strain curve will be similar to that of its previous unloading: a reduced initial stress response with strain hardening occurring as the specimen's maximum previous load is achieved. Straining the sample further continues the response seen in the virgin material, as well as alters its response to future loadings (by adjusting the maximum previous load). This effect was found to be permanent, correlating

to inelastic elongation of the specimens at these high strains. Additionally, it mirrors the same hysteretic response observed in the electrical properties, with the maximum previous mechanical load determining the subsequent volumetric conductivity. This observation provides further evidence for the postulate that deformation of the PDMS–galinstan composite alters its interior structure. The elastic modulus measured up to 10% strain of the virgin material was measured to be 1.27 MPa. If the sample had been previously strained to 100% its original length, this 10% strain modulus drops to 0.90 MPa (Figure 3g). Compressing the material to induce conductivity is believed to cause a similar decrease. When compared with the Young's modulus of plain PDMS (2.59 MPa when cured at 150 °C[38]), adding galinstan decreases the stiffness. This is not surprising since the liquid inclusions make up 50% of the composite volume and should have negligible mechanical resistance to stretch. Elongation at break was found to be $\varepsilon_f = 133\%$ strain on average, allowing for high stretchability in devices made with this material.

To highlight the ability to selectively induce conductivity, we have created a variety of simple circuits using a ball point pen (0.8 mm diameter; 3.6 MPa of required pressure) and a square-shaped sample of the composite. Electrical terminals and interconnects can be formed by drawing lines onto the surface of the sample, as seen for the LED circuit in Figure 1c–f. Connections made in this way have low electrical resistance due the material's high conductivity. Multiple unconnected traces on a single sheet of the material can also function as a capacitor (Video S1, Supporting Information), as electricity is not transferred through the noncompressed region of the material. Spiral geometries can be used if inductance is desired, as seen in Video S2, Supporting Information. Circuits created in this fashion should be protected by casting a thick layer of soft polymer on the top and bottom surface, so that compressive forces dissipate, reducing stress concentrations which can induce conductivity in unwanted regions. Stencil lithography can also be utilized to deposit patterned layers of the PDMS–galinstan to create circuits (Figure S2, Supporting Information), as done with other conductive polymer composites.

In conclusion, we have introduced a new form of conductive stretchable material by combining two approaches already commonly used for compliant electronics: conductive elastomer composites and liquid metal microfluidics. The PDMS–galinstan composite demonstrates the unique advantages of this approach, resulting in high stretchability and good electrical conductivity. This comes from galinstan's liquid state, which preserves the elastic nature of the surrounding PDMS matrix and leads to a net decrease in the effective tensile modulus of the composite. Volumetric conductivity is observed to increase with stretch, offsetting the increase in resistance that would otherwise arise from elongation and reduced cross-sectional area during tensile loading. PDMS–galinstan is highly accessible, requiring minimal equipment for manufacturing the material and, as with other polymer composites, simple rapid patterning techniques are easily applicable. The requirement to apply concentrated surface pressure in order to induce conductivity allows for selective conductivity. For applications that require homogenous conductivity, the elastomer can be pressed with a rigid roller. This "postprocessing" step for initializing conductivity can potentially be avoided by introducing additional conductive particles that would form electrical connections between isolated droplets.

Experimental Section

Material Fabrication and Specimen Preparation: PDMS (Sylgard 184; Dow Corning Corporation) was prepared at a 10:1 weight ratio (base:curing argent) and then added to a 4 oz. glass mortar. Galinstan (Ga 68.5%, In 21.5%, Sn 10% by weight; GalliumSource, LLC) was then added to the mortar at a 1:1 volume ratio (6.6 Galinstan:1 PDMS wt. ratio) to the PDMS and mixed gently with a pestle until all of the liquid metal was encapsulated within the polymer. More vigorous mixing was applied (≈15 min) to reduce the droplets to below to the desired size (2–30 μm), that size confirmed using an optical microscope. Specimens were prepared using stencil lithography (mask deposition). LaserTape (Ikonics Imaging) and backing were patterned using a laser cutter (VLS3.50; 2.0 lens, 6.2% power, 5% speed, 500 ppi; Universal Laser Systems, Inc.) and placed tape-side down onto a metal substrate prepared with Ease Release 200 (Mann Formulated Products, Inc.) mold release. A ZUA 2000 Universal Applicator (Zehntner Testing Instruments) was used to distribute the PDMS–galinstan material over the LaserTape mask. Afterward, the mask was removed and the metal substrate was placed on a hot plate set to 150 °C to cure for at least 1 h. Specimens could then be removed with tweezers. Some demo specimens were fabricated with a 100 μm layer of PDMS on the top and bottom surface, this layer deposited before and after the composite using a ZUA 2000 thin-film applicator. An alternate fabrication method using sonication is described in the Supporting Information. Conductivity was induced by placing a sample between two 0.05 mm sheets of copper and pressing a 9.5 mm steel rod and rolling it along the surface, or using a ball-point pen directly on the surface to target select regions.

Thickness Measurement: The material deposited by the thin-film applicator could be thinner than that indicated due to its viscosity. We verified the thickness by measuring it using a Newport 460A-X actuator, custom 3D-printed probe (VeroWhitePlus plastic; Objet24; Stratasys Ltd.) with square 5 mm area, and digital scale (L-600, Escali Corp). The actuator and probe were used to place a small load on the sample to demonstrate contact, using 5 g as the cutoff for contact to ensure the sample was flat against the scale.

Measuring Compression Required for Conductivity: Compression was applied using a 3.2 mm diameter dowel pin as a probe and a manual linear actuator (A1506Q2-S1.5; Velmex, Inc.) or with a pen ink cartridge (Hub Pen 11H, 0.8 mm tip) pushed into the surface by hand. A Scout Pro SP2001 (OHAUS) scale located beneath the sample was used to measure the force applied. A BK Precision model 889B bench LCR/ESR meter connected to the probe and a sheet of 0.05 mm copper under the sample were used to record the resistance. Samples were circular with a diameter of 9 mm and thicknesses ≈0.50 mm.

Conductivity as a Function of Tensile Strain: Velmex manual linear actuators were used to stretch samples clamped into textured 3D printed grips. The sample ends within the clamps were sandwiched between folded 0.05 mm copper sheets, which were connected to a BK Precision LCR/ESR meter to record the resistance. Specimens were 3 mm × 25 mm with square ends and thicknesses 0.17–0.20 mm. Samples were compressed as described in fabrication.

Mechanical Tensile Testing: Mechanical characterization was performed using a model 4442 Instron, loading and unloading the samples at 10 mm min^{-1}. Special textured insets were fabricated using 3D printing. Specimens were 5 mm × 50 mm with square ends and thicknesses between 0.19 and 0.24 mm.

Supporting Information

Supporting Information is available from the Wiley Online Library or from the author.

Acknowledgements

[1] S. Cheng, Z. Wu, *Lab Chip* **2012**, *12*, 2782.

[2] P. G. Agache, C. Monneur, J. L. Leveque, J. De Rigal, *Arch. Dermatol. Res.* **1980**, *269*, 221.

[3] I. W. Hunter, S. Lafontaine, *IEEE Solid-State Sens. Actuator Workshop* **1992**, *5*, 178.

[4] D. W. G. Jung, T. Blange, H. De Graaf, B. W. Treijtel, *Biophys. J.* **1988**, *54*, 897.

[5] X. Z. Niu, S. L. Peng, L. Y. Liu, W. J. Wen, P. Sheng, *Adv. Mater.* **2007**, *19*, 2682.

[6] H. Cong, T. Pan, *Adv. Funct. Mater.* **2008**, *18*, 1912.

[7] M. A. Unger, H.-P. Chou, T. Thorsen, A. Scherer, S. R. Quake, *Science* **2000**, *288*, 113.

[8] D. H. Kim, N. Lu, R. Ma, Y. S. Kim, R. H. Kim, S. Wang, J. Wu, S. M. Won, H. Tao, A. Islam, K. J. Yu, T. Kim, R. Chowdhury, M. Ying, L. Xu, M. Li, H.-J. Chung, H. Keum, M. McCormick, P. Liu, Y. W. Zhang, F. G. Omenetto, Y. Huang, T. Coleman, J. Rogers, *Science* **2011**, *333*, 6044.

[9] L. Xu, S. R. Gutbrod, A. P. Bonifas, Y. Su, M. S. Sulkin, N. Lu, H. J. Chung, K. I. Jang, Z. Liu, M. Ying, C. Lu, R. C. Webb, J.-S. Kim, J. I. Laughner, H. Cheng, Y. Liu, A. Ameen, J. W. Jeong, G. T. Kim, Y. Huang, I. R. Efimov, J. Rogers, *Nat. Commun.* **2014**, *5*, 3329.

[10] S. Xu, Y. Zhang, J. Cho, J. Lee, X. Huang, L. Jia, J. A. Fan, Y. Su, J. Su, H. Zhang, H. Cheng, B. Lu, C. Yu, C. Chuang, T. I. Kim, T. Song, K. Shigeta, S. Kang, C. Dagdeviren, I. Petrov, P. V. Braun, Y. Huang, U. Paik, J. Rogers, *Nat. Commun.* **2013**, *4*, 1543.

[11] I. Jung, J. Xiao, V. Malyarchuk, *Proc. Natl. Acad. Sci. USA* **2011**, *108*, 2011.

[12] C. Majidi, Y. L. Park, R. Kramer, P. Bérard, R. J. Wood, *J. Micromech. Microeng.* **2010**, *20*, 125029.

[13] A. Fassler, C. Majidi, *Smart Mater. Struct.* **2013**, *22*, 55023.

[14] C. Majidi, R. Kramer, R. J. Wood, *Smart Mater. Struct.* **2011**, *20*, 105017.

[15] G. J. Hayes, A. Qusba, M. D. Dickey, G. Lazzi, *IEEE Trans. Antennas Propag.* **2012**, *60*, 2151.

[16] S. Cheng, Z. Wu, *Lab Chip* **2010**, *10*, 3227.

[17] L. R. Finkenauer, C. Majidi, *Proc. SPIE* **2014**, *9056*, 90563I.

[18] M. R. Khan, C. B. Eaker, E. F. Bowden, M. D. Dickey, *Proc. Natl. Acad. Sci. USA* **2014**, *111*, 14047.

[19] R. Verdejo, M. M. Bernal, L. J. Romasanta, M. A. Lopez-Manchado, *J. Mater. Chem.* **2011**, *21*, 3301.

[20] Q. Xu, N. Oudalov, Q. Guo, H. M. Jaeger, E. Brown, *Phys. Fluids* **2012**, *24*, 63101.

[21] R. J. Larsen, M. D. Dickey, G. M. Whitesides, D. A. Weitz, *J. Rheol.* **2009**, *53*, 1305.

[22] M. D. Dickey, R. C. Chiechi, R. J. Larsen, E. A. Weiss, D. A. Weitz, G. M. Whitesides, *Adv. Funct. Mater.* **2008**, *18*, 1097.

[23] A. Tabatabai, A. Fassler, C. Usiak, C. Majidi, *Langmuir* **2013**, *29*, 6194.

[24] J. H. So, M. D. Dickey, *Lab Chip* **2011**, *11*, 905.

[25] C. Ladd, J. H. So, J. Muth, M. D. Dickey, *Adv. Mater.* **2013**, *25*, 5081.

[26] M. Knite, V. Teteris, A. Kiploka, J. Kaupuzs, *Sens. Actuators A* **2004**, *110*, 142.

[27] A. Kaskela, A. G. Nasibulin, M. Y. Timmermans, B. Aitchison, A. Papadimitratos, Y. Tian, Z. Zhu, H. Jiang, D. P. Brown, A. Zakhidov, E. I. Kauppinen, *Nano Lett.* **2010**, *10*, 4349.

[28] M. Chen, T. Tao, L. Zhang, W. Gao, C. Li, *Chem. Commun.* **2013**, *49*, 1612.

[29] D. J. Lipomi, M. Vosgueritchian, B. C. K. Tee, S. L. Hellstrom, J. A. Lee, C. H. Fox, Z. Bao, *Nat. Nanotechnol.* **2011**, *6*, 788.

[30] K. Y. Chun, Y. Oh, J. Rho, J.-H. Ahn, Y.-J. Kim, H. R. Choi, S. Baik, *Nat. Nanotechnol.* **2010**, *5*, 853.

[31] M. Park, J. Im, M. Shin, Y. Min, J. Park, H. Cho, S. Park, M.-B. Shim, S. Jeon, D. Y. Chung, J. Bae, J. Park, U. Jeong, K. Kim, *Nat. Nanotechnol.* **2012**, *7*, 803.

[32] S. Merilampi, T. Björninen, V. Haukka, P. Ruuskanen, L. Ukkonen, L. Sydänheimo, *Microelectron. Reliab.* **2010**, *50*, 2001.

[33] T. Akter, W. S. Kim, *ACS Appl. Mater. Interfaces* **2012**, *4*, 1855.

[34] S. Y. Fu, X. Q. Feng, B. Lauke, Y. W. Mai, *Composites, Part B* **2008**, *39*, 933.

[35] S. Ahmed, F. Jones, *J. Mater. Sci.* **1990**, *25*, 4933.

[36] B. J. Blaiszik, S. L. B. Kramer, M. E. Grady, D. A. McIlroy, J. S. Moore, N. R. Sottos, S. R. White, *Adv. Mater.* **2012**, *24*, 398.

[37] J. Park, S. Wang, M. Li, C. Ahn, J. K. Hyun, D. S. Kim, D. K. Kim, J. A. Rogers, Y. Huang, S. Jeon, *Nat. Commun.* **2012**, *3*, 916.

[38] I. D. Johnston, D. K. McCluskey, C. K. L. Tan, M. C. Tracey, *J. Micromech. Microeng.* **2014**, *24*, 1.